arXiv:1107.4831v1 [astro-ph.HE] 25 Jul 2011

Mon. Not. R. Astron. Soc. **000**, 000–000 (0000) Printed 26 July 2011 (MN LaTeX style file v2.2)

Modelling interaction of relativistic and non-relativistic winds in binary system PSR B1259-63/SS2883* - II. Impact of magnetization and anisotropy of the pulsar wind

Bogovalov[1] S.V.,Khangulyan[2] D.,Koldoba[3] A.V.,Ustyugova[3] G.V.,Aharonian[4,5] F.A.

[1] *Moscow Engineering Physics Institute (state university), Moscow, Russia,*

[2] *Institute of Space and Astronautical Science/JAXA, Sagamihara, Japan,*

[3] *Keldysh Institute of Applied Mathematics RAS, Moscow, Russia,*

[4] *Dublin Institute for Advanced Studies, Dublin, Ireland,*

[5] *Max-Planck-Institut für Kernphysik, Heidelberg, Germany.*

ABSTRACT

In this paper, we present a numerical study of the properties of the flow produced by the collision of a magnetized anisotropic pulsar wind with its environment in binary system. We compare the impact of both the magnetic field and the wind anisotropy to the benchmark case of a purely hydrodynamical (HD) interaction of isotropic winds, which has been studied in detail by Bogovalov et al. (2008). We consider the interaction in axisymmetric approximation, i.e. the pulsar rotation axis is assumed to be oriented along the line between the pulsar and the optical star and the effects related to the pulsar orbiting are neglected. The impact of the magnetic field is studied for the case of weak magnetization (with magnetization parameter $\sigma < 0.1$), which is consistent with conventional models of pulsar winds. The effects related to anisotropy in pulsar winds are modeled assuming that the kinetic energy flux in a non-magnetized pulsar wind is strongly anisotropic, with the minimum at the pulsar rotation axis and the maximum in the perpendicular direction. We show that, although both considered effects change the shape of the region occupied by the terminated pulsar wind, their impact appears to be small.

---

* Star SS2883 in what follows will be refereed as LS2883 according to the standard catalog of Luminous Stars in the Southern Milky Way (Stephenson & Sanduleak 1971)

In particular, for the magnetization of the pulsar wind below 0.1, the magnetic field pressure remains well below the plasma pressure in the post-shock region. Thus, in the case of interaction of a pulsar with the stellar wind environment (opposite to the case of plerions, i.e. the pulsar interaction with the interstellar medium, when the magnetic field becomes dynamically important independently on the wind magnetization) the HD approach represents a feasible approximation for numerical modelling.

Key words: HD – shock waves - pulsars: binaries.

1 INTRODUCTION

Pulsars lose their rotation energy through relativistic winds, the interaction of which with the surrounding environment leads to the formation of so-called Pulsar Wind Nebulae (PWNe). PWNs are bright in X- and gamma ray regions filled with ultrarelativistic electrons accelerated at the pulsar wind termination shock (Rees & Gunn 1974; Kennel & Coroniti 1984a). While Crab Nebula is the most famous (although rather atypical) representative, the recent X-ray and TeV gamma ray observations have shown (see e.g. Gaensler & Slane 2006) that the formation of PNWe is a common phenomenon for many other pulsars as well. Importantly, the physical conditions, and consequently their observational properties, appear to differ significantly in different PWNs. A very interesting situation arises when a pulsar is located in a binary system. In this case the pulsar wind interacts with the wind from the companion star. This case, in particular, is realized in the binary system PSR1259-63/LS2883 which consists of a $\sim$ 47.8ms pulsar in an elliptic orbit, with eccentricity $e = 0.87$, around a massive fast rotating O8 optical companion (Johnston et al. 1992; Negueruela et al. 2011). Observations show that this system is a strongly variable source of non-thermal emission extending from radio to TeV gamma-rays (see e.g. Neronov & Chernyakova 2007, and references therein).

Two other variable TeV galactic gamma-ray sources, LS 5039 and LS I +61 303 (see e.g. Paredes et al. 2000; Bosch-Ramon & Khangulyan 2009), are discussed as possible, although less evident candidates for being a part of a “binary pulsar” source population (Maraschi & Treves 1981; Martocchia et al. 2005). LS 5039 consists of an O6.5V star and an unidentified compact object in a 3.9 days orbit. This object has been detected as a periodic source of gamma rays by HESS (Aharonian et al. 2006, 2005) and by *Fermi* Large Area Telescope (LAT) (Abdo et al. 2009). In LS I +61 303 an unidentified compact source moves around a B0Ve star in an eccentric orbit with a period of 26.5 days. This source was as well detected in GeV and TeV gamma rays (Albert et al. 2006; Abdo et al. 2009; Anderhub et al. 2009; Acciari et al. 2011). Although, the compact source nature in these objects (black hole or neutron star) is not yet firmly established, the binary pulsar scenario provides a possible explanation of the broadband non-thermal emission detected from these sources (see e.g. Dubus 2006).

The collision of supersonic winds from two stars located in a binary system results in formation of two terminating shock fronts and a tangential discontinuity separating relativistic and nonrelativistic parts of the shocked flow. It has been found from the detailed hydrodynamical modelling (Bogovalov et al. 2008) that the shocked flow propagates into a limited solid angle with rather high velocity. It has been shown that on the scales, which characterize the binary system, the shocked pulsar wind material obtains relativistic bulk velocities. As proposed by Khangulyan et al. (2008), this should lead to the formation of strongly variable non-thermal emission due to the Doppler boosting, thus a detailed study of the properties of the post-shock flow is important for proper interpretation of variable X- and gamma rays detected from the system (Aharonian et al. 2005b; Chernyakova et al. 2006; Uchiyama et al. 2009; Aharonian et al. 2009; Abdo et al. 2011).

In the previous pure HD study by Bogovalov et al. (2008) several potentially important effects have been identified for the future research. In particular, the development of Kelvin-Helmholtz instability at the contact discontinuity and orbital motion of the pulsar should enhance the mixing of pulsar and stellar wind materials on a spacial scales slightly exceeding the size of the binary system (Bosch-Ramon & Barkov 2011). Given relatively short cooling time of VHE electrons (see e.g. Khangulyan et al. 2007) this mixing should not significantly affect the variable gamma ray component, which is expected to be produced inside the system. On the other hand, several other effects related to impact of magnetic field and anisotropy of the pulsar wind, which are almost unavoidable features of the pulsar wind, appear to be important already on the scales of binary system. The importance of this effects can be illustrated by the impact of the magnetic field on the interaction of the pulsar wind with interstellar medium. Even a weak magnetization of the pulsar wind can result in a dramatic modification of the flow in the post shock region (Komissarov & Lyubarsky 2003; Bogovalov et al. 2005; Bucciantini et al. 2005). In this paper we present a study of the role of the magnetic field and anisotropic energy flux on the dynamic of the shocked material in binary pulsar systems.

2 PROPERTIES OF THE PULSAR AND STELLAR WINDS OF PSR B1259-63/SS2883

The separation distance between the pulsar and optical star in PSR-B1259-63/LS2883 changes by more than order of magnitude depending on the orbital phase. Consequently, the physical conditions at the interaction point can vary significantly. While the processes related to particle acceleration and radiation may be strongly affected by change of the separation distance (see e.g. Khangulyan et al. 2007), the regime of hydrodynamical interaction of the stars depends weakly on this parameter. Indeed, since the interaction of the winds depends on the ratio of the ram pressures of the winds, collision regime remains unaffected by the change of the separation distance, unless the stellar wind undergoes a significant acceleration or pulsar wind suffers a strong Compton drag (see e.g. Khangulyan et al. 2007). Finally, the interaction at different orbital phases may differ significantly due to presence of dense stellar disk in the system.

2.1 Parameters of the pulsar wind

Spin-down luminosity of the pulsar PSR B1259-63 is $L_{sd} = 8 \times 10^{35}\mathrm{erg\,s^{-1}}$. This energy is released in the form of electromagnetic and kinetic energy fluxes carried away by pulsar wind. Magnetic field in the wind may be represent as superposition of two components with essentially different spatial dependencies: the poloidal magnetic field component decreases with radius as r^{-2}, while the toroidal magnetic field has a weaker dependence, namely proportional to r^{-1}. Thus, at distances larger than light cylinder radius the toroidal magnetic field strongly dominates over the poloidal one. Therefore, only the toroidal magnetic field component has been taken into account in the modelling. To keep axial symmetry in the model the axis of rotation of the pulsar is assumed to be directed along the line connecting the pulsar and optical star. Figure 1 shows a schematic representation of the wind interaction geometry.

The magnetic field strength is characterized by the magnetization parameter σ, which is the ratio of the magnetic field energy to kinetic energy fluxes. Conventional theories of plasma generation in pulsar magnetospheres predict a highly magnetized wind with $\sigma \gg 1$ at the light cylinder. In this case the energy flux from pulsar is not isotropic and is expected to have the following form

$$\frac{\mathrm{d}L}{\mathrm{d}\Omega} = \gamma_0 mc^2 \frac{\mathrm{d}N}{\mathrm{d}\Omega} + P_0 \sin^2(\theta)\,. \tag{1}$$

Here $P_0 \sin^2(\theta)$ is the Pointing flux obtained in the frameworks of the split-monopole model (Bogovalov 1999); $\frac{\mathrm{d}N}{\mathrm{d}\Omega}$ is the particle flux in the wind; and θ is the angle between the pulsar rotational axis and direction of the flow. Obviously, in this case the ratio of the Poynting flux to the kinetic energy density flux varies with θ. It is convenient to define σ as the ratio $P_0/(\gamma_0 mc^2 \frac{\mathrm{d}N}{\mathrm{d}\Omega})$ which equals to the ratio of the Poynting flux to the kinetic energy flux in the equatorial plane of the pulsar wind.

Interpretation of observations usually leads to the conclusion that the wind energy flux at large distances from the pulsar is concentrated in the particle kinetic energy, i.e. $\sigma \ll 1$ (Kennel & Coroniti 1984b). Thus, a transformation of the Poynting flux to the pulsar wind bulk motion is to occur in the pulsar wind zone, although we note that the physical mechanism responsible for this transformation still remains unknown. Assuming that the most of the Poynting flux is transformed into the kinetic energy flux, Eq. (1) can be rewritten as

$$\frac{\mathrm{d}L}{\mathrm{d}\Omega} = \gamma_0 mc^2 \frac{\mathrm{d}N}{\mathrm{d}\Omega} + \gamma_{\max} \sin^2(\theta) mc^2 \frac{\mathrm{d}N}{\mathrm{d}\Omega} + P \sin^2(\theta)\,, \tag{2}$$

where we assumed that the particle flux $\frac{\mathrm{d}N}{\mathrm{d}\Omega}$ is isotropic. Then the σ parameter equals to the ratio $P/(\gamma_{\max} mc^2 \frac{\mathrm{d}N}{\mathrm{d}\Omega})$. We should note that the original definition of σ in Kennel & Coroniti (1984b) does not differ essentially from the one used here given that $\gamma_{\max} \gg \gamma_0$. According to this definition σ parameter is the fraction of the initial Poynting flux remaining in the electromagnetic form at the wind termination shock.

Thus, the requirement of a kinetically dominated pulsar wind leads to the conclusion that the wind should be strongly anisotropic and weakly magnetized. To study the impact of these effects, below we consider two different models: (i) weakly magnetized isotropic wind; and (ii) highly anisotropic unmagnetized wind.

2.2 Parameters of the stellar wind

Given the fast rotation of LS2883, the stellar wind is believed to have a strong angular dependence. Namely, it is expected that the stellar outflow consists of two parts with comparable mass loss rates: an almost isotropic polar wind and a dense Keplerian disk in the plane perpendicular to the star rotation axis. The mass loss rate and velocity profiles of stellar winds is a subject of future dedicated studies. We note however that although the precise measurements presently are not available, the properties of the wind can be estimated based on the luminosity and temperature of the star (Vink et al. 2000). The physical

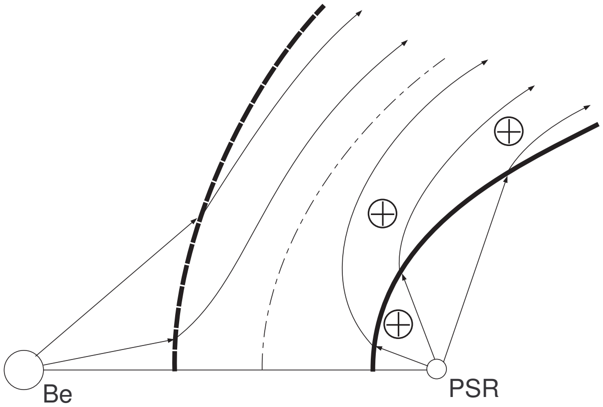

Figure 1. The scheme of the wind interaction and the post shock flow. The flow from optical star is terminated by the nonrelativistic shock front (thick dashed line). The flow from the pulsar is terminated by the relativistic shock front (thick solid line). Nonrelativistic and relativistic post shock flows are separated by the contact discontinuity (dashed-dotted line). The symbol ⊕ shows the direction of the toroidal magnetic field which has been assumed to exist only in the region occupied by pulsar wind.

characteristics of the optical star LS2883 have been recently significantly revised towards higher temperature and luminosity (Negueruela et al. 2011). This leads consequently to a higher mass loss rates. In particular, the mass loss rate of the polar wind is expected to be at the level of $\dot{M} = 6 \times 10^{-8} M_{\odot} \mathrm{yr}^{-1}$ (Negueruela et al. 2011), which exceeds significantly the rate assumed in the previous study by Bogovalov et al. (2008). Thus, the expected ratio of the winds ram pressures, η parameter, for the case of the interaction of the pulsar wind with the stellar polar wind is as follows:

$$\eta = \frac{L_{\mathrm{sd}}}{\dot{M} c V_{\mathrm{w}}} = 5 \times 10^{-2} \left(\frac{\dot{M}}{6 \times 10^{-8} M_{\odot} \mathrm{yr}^{-1}} \right)^{-1} \left(\frac{V_{\mathrm{w}}}{1350\,\mathrm{km\,s^{-1}}} \right)^{-1}, \quad (3)$$

where the wind velocity has been normalized to the value of the wind termination velocity $V_{\mathrm{inf}} = 1350 \pm 200\,\mathrm{km\,s^{-1}}$ (McCollum 1993).

Since a rather broad range of variation of the η parameter has been discussed in the previous study by Bogovalov et al. (2008), here we adopt two values of η: $\eta = 0.05$ and $\eta = 0.1$, which are similar to the estimate given by Eq. (3).

3 BASIC ASSUMPTIONS.

The evolution of the flow due to the change of the star separation distance is assumed to be adiabatic, i.e. we consider the collision of the winds as a steady process. All factors resulting in time-dependent effects were ignored or intentionally suppressed. In particular, the tangential instability arising at the interface between the relativistic and nonrelativistic flows in the post shock region is suppressed (Bogovalov et al. 2008). The rotation axis of the pulsar was assumed to be co-directed with the line connecting the pulsar and the optical star, thus the flow in the computational domain was considered as axisymmetric in respect to this line. It implies that all effects related to the orbiting of the pulsar are ignored, although these effects may appear to be very important on larger scales (Bosch-Ramon & Barkov 2011).

The Lorentz factor of the particles in the pulsar wind is expected to be very high, $\gamma_{\max} \sim 10^6$ (Bogovalov & Khangoulian 2002). Remarkably, the post shock flow practically does not depend on $\gamma_{\max}$ provided that $\gamma_{\max} \gg 1$. Almost all the energy of the bulk motion is transformed into "thermal" energy of plasma, thus it is possible to neglect the rest mass energy of the electrons compare with the thermal energy and the particle density is not present in the equations describing the motion of the relativistic pulsar wind in the post shock region.

4 METHOD OF SOLUTION

A special numerical method was used for the integration of the transient HD (hydrodynamical) and RMHD (relativistic magnetohydrodynamical) equations (Ustyugova et al. 1999). The integration of the HD equations was performed in the region limited by the non-relativistic termination shock and the contact discontinuity. The RMHD equations were integrated in the region located between the relativistic termination shock and the contact discontinuity. The plasma flow outside these two regions corresponds to a supersonic pulsar and a stellar wind, i.e. it has been considered as known. The modelling has been performed with the use of an adaptive computational mesh (see for details Bogovalov et al. 2008). In the region occupied by the shocked relativistic plasma the RMHD equations in cylindrical coordinates are

$$\frac{\partial n\gamma}{\partial t} + \frac{1}{r}\frac{\partial r n\gamma v_r}{\partial r} + \frac{\partial n\gamma v_z}{\partial z} = 0. \tag{4}$$

$$\frac{\partial \gamma^2(w+h^2)v_r}{\partial t} + \frac{1}{r}\frac{\partial}{\partial r} r\left((w+h^2)\gamma^2 v_r^2 + (p+\frac{h^2}{2})\right) + \\ + \frac{\partial}{\partial z}(w+h^2)\gamma^2 v_r v_z = \frac{p+\frac{h^2}{2}}{r}. \tag{5}$$

$$\frac{\partial \gamma^2(w+h^2)v_z}{\partial t} + \frac{1}{r}\frac{\partial}{\partial r} r(w+h^2)\gamma^2 v_r v_z + \\ + \frac{\partial}{\partial z}\left((w+h^2)\gamma^2 v_z^2 + (p+\frac{h^2}{2})\right) = 0. \tag{6}$$

$$\frac{\partial}{\partial t}\left(\gamma^2(w+h^2)-(p+\frac{h^2}{2})\right)+\frac{1}{r}\frac{\partial}{\partial r}r(w+h^2)\gamma^2 v_r + \\ +\frac{\partial}{\partial z}(w+h^2)\gamma^2 v_z = 0. \tag{7}$$

$$\frac{\partial h\gamma}{\partial t}+\frac{\partial h\gamma v_r}{\partial r}+\frac{\partial \gamma v_z h}{\partial z}=0\ . \tag{8}$$

Here p, $w=\frac{4}{3}p$, n and h are the pressure, enthalpy density, particle density and magnetic field, respectively (all quantities are in the local rest frame); v_r, and v_z are the components of the flow velocity.

In the region occupied by the shocked nonrelativistic plasma the equations are

$$\frac{\partial\rho}{\partial t}+\frac{1}{r}\frac{\partial r\rho v_r}{\partial r}+\frac{\partial \rho v_z}{\partial z}=0 \tag{9}$$

$$\frac{\partial\rho v_r}{\partial t}+\frac{1}{r}\frac{\partial}{\partial r}r\left(\rho v_r^2+p\right)+\frac{\partial}{\partial z}\rho v_r v_z=\frac{p}{r} \tag{10}$$

$$\frac{\partial\rho v_z}{\partial t}+\frac{1}{r}\frac{\partial}{\partial r}r\rho v_r v_z+\frac{\partial}{\partial z}\left(\rho v_z^2+p\right)=0 \tag{11}$$

$$\frac{\partial}{\partial t}\left(\frac{\rho v^2}{2}+\epsilon\right)+\frac{1}{r}\frac{\partial}{\partial r}r v_r\left(\frac{\rho v^2}{2}+\epsilon+p\right)+ \\ +\frac{\partial}{\partial z}v_z\left(\frac{\rho v^2}{2}+\epsilon+p\right)=0 \tag{12}$$

Here ρ and ϵ are the densities of the mass and the thermal energy, respectively, and $p=2/3\epsilon$ is the pressure. The computational method used in this work has been developed earlier for the solution of the equation describing the interaction of a magnetized relativistic pulsar wind with the interstellar medium (see for details Bogovalov et al. 2005, 2008).

5 RESULTS

5.1 Impact of magnetic field

To investigate the impact of the magnetic field on the process of the winds collision, a sequence of calculations are performed for different values of the σ parameter and a fixed value of $\eta=0.1$. The range of considered σ parameter has been chosen to be $\sigma=0.003-0.1$, which corresponds to the conventional magnetization of the pulsar wind. As mentioned above, the solution in the hydrodynamical limit ($\sigma=0$) was obtained earlier by Bogovalov et al. (2008).

In Figure 2 the total pressure distribution (i.e. both gas and magnetic field pressures $p+h^2/2$) together with stream lines are shown for different pulsar wind magnetizations. A similar distribution obtained for the case of an unmagnetized pulsar wind is shown in

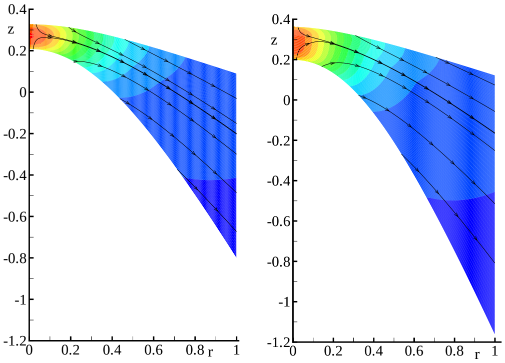

Figure 2. Distribution of total pressure and stream lines in the post shock region for two different values of the magnetization of the pulsar wind: $\sigma = 0.03$(left panel) and $\sigma = 0.1$ (right panel). The ratio of the winds ram pressures was assumed to be $\eta = 0.1$.

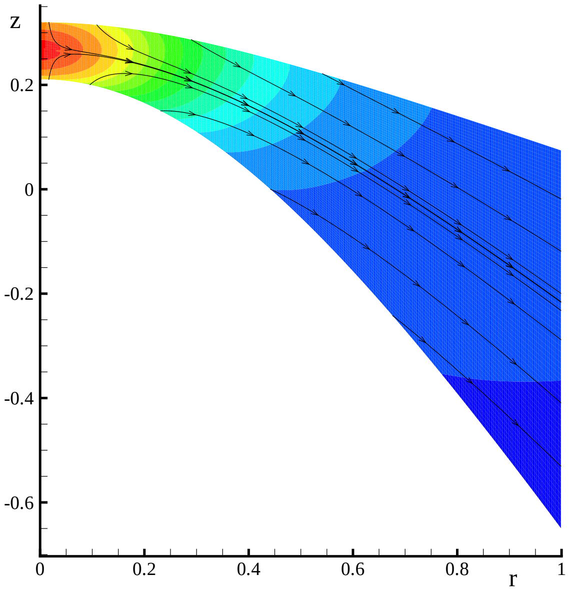

Figure 3. Distribution of total pressure and stream lines in the post shock region for the unmagnetized pulsar wind, i.e. $\sigma = 0$. The ratio of the winds ram pressures was assumed to be $\eta = 0.1$.

Fig. 3. A comparison of these figures shows that the impact of the magnetic field on the post shock flow is rather weak. The magnetic field collimates the post shock flow toward the axis. This happens due to the pinching of the flow by the toroidal magnetic field (see e.g. Bogovalov & Tsinganos 1999).

5.2 Anisotropy of the pulsar wind

As it has been described above, we study the impact of an anisotropic energy flux in the pulsar wind under the approximation of an unmagnetized wind. Thus, we have introduced a polar angle dependence of the pulsar wind bulk Lorentz factor: $\gamma = \gamma_0 + \gamma_{\max} \sin^2 \theta$, where γ_0 is the initial Lorentz factor of the wind in the direction of the rotation axis; and $\gamma_{\max}$

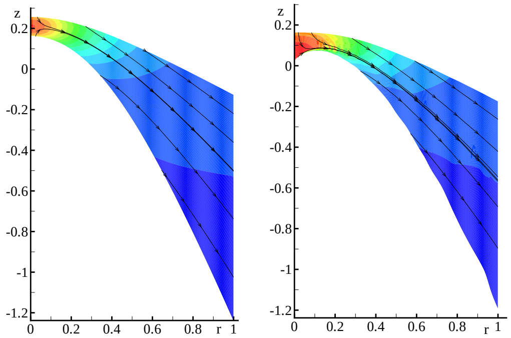

Figure 4. Gas pressure and stream lines in the post shock region for the isotropic pulsar wind with $\eta = 0.05$ (left panel) and anisotropic wind with $< \eta >= 0.05$ and $a = 100$ (right panel).

is the wind Lorentz factor at the equator. It is expected that the pulsar wind is strongly anisotropic, i.e. $\gamma_{\max} \gg \gamma_0$. The level of anisotropy can be characterized by the ratio of polar and equatorial Lorentz factors: $a = \gamma_{\max}/\gamma_0$. In the calculations we adopted a value of $a = 100$. The definition of the η parameter should be modified in the case of an anisotropic pulsar wind. Namely, it is natural to assign it to the ram pressure ratio averaged over the polar angle, i.e. $< \eta >$.

In Figure 4, a comparison of the pressures and stream lines is shown for two cases: isotropic pulsar wind with $\eta = 0.05$ and anisotropic pulsar wind with $< \eta >= 0.05$ and $a = 100$. It might be seen from the figure that the relativistic terminal shock is located closer to the pulsar at the axis. This happens because the momentum flux in this direction is much smaller than the averaged one. It might be seen as well, that in the case of an anisotropic pulsar wind, the tangential instability is somewhat more pronounced. In particular, this is visible on the shape of the pulsar wind termination shock. Beside these minor changes the geometry of the flow, in the region down stream farther from the axis, is similar to the flow produced by an isotropic winds.

6 DISCUSSION AND CONCLUSIONS

The present study of the interaction of a pulsar and a stellar winds within the framework of an MHD approach shows that the magnetic field has a rather small impact on the post shock flow. The only apparent effect revealed by MHD consideration, compared to a pure HD treatment, is weak collimation of the relativistic flow towards the axis. This conclusion is in strong contrast with the case of plerions, i.e. when the pulsar wind interacts with the interstellar medium (Bucciantini 2002; Khangoulian & Bogovalov 2003; Komissarov & Lyubarsky 2003;

Bogovalov et al. 2005). In the case of plerions even a weak seed toroidal field results in efficient collimation of the post shock flow. This difference has a rather fundamental reason illustrated in Fig. 6, where the distribution of the bulk motion Lorentz factor is shown. As it is seen from this figure, the bulk Lorentz factor is increasing in the downstream region, i.e. physically the wind collision geometry acts as a nuzzle, providing an efficient bulk acceleration of the plasma in the post shock flow. The shock pulsar wind velocity fast reaches relativistic values downstream the shock. It implies an inefficient collimation of the plasma, which is a rather general effect for relativistic outflows (Bogovalov & Tsinganos 1999). In contrast to this case, if the pulsar wind collides with homogeneous medium (i.e. interstellar gas), a flow deceleration occurs in the post shock region. This results into a few effects making magnetic collimation to be very efficient (Khangoulian & Bogovalov 2003). The inertia of the plasma decreases with a decrease of the velocity, thus it is easier to change the direction of the flow even by a small force. Additionally, since in this case the flow is subsonic, the toroidal magnetic field increases with the distance from the shock. For this reason even a weak initial field is amplified quickly and can provide an efficient collimation of the flow towards the axis.

The impact of the pulsar wind magnetization and anisotropy is investigated for case of the collision of the pulsar wind with the non-relativistic wind from a massive star. It is shown, that the magnetic field leads to weak collimation of the post shock flow toward the axis. The effect remains very weak for a broad parameter range, in particular for the strongest considered magnetization of $\sigma = 0.1$. This weak impact of the magnetic field on the wind collision is the result of the acceleration of the plasma bulk motion due to adiabatic cooling. This implies that the calculation of the radiation produced at the wind collision can be performed in the hydrodynamical limit in which the toroidal magnetic field is calculated as a passive scalar not affecting dynamics of the plasma.

The influence of anisotropy of the pulsar wind appeared as well to be small. Whereas its impact can be seen on the shape of the pulsar wind termination shock and the enhanced potential rate of instabilities, the general structure of the flow remains almost identical to the case of isotropic pulsar wind. Although, we note that in the case of a different orientation of the pulsar equatorial plane, a stronger effect can arise.

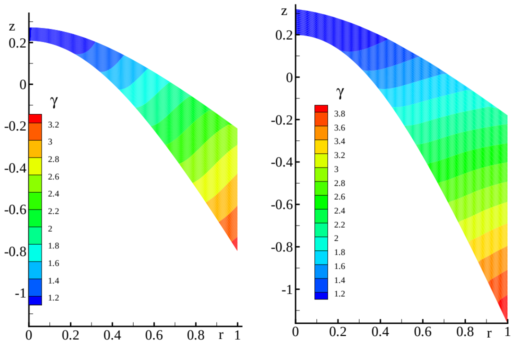

Figure 5. Lorentz factor in the post shock region of the isotropic pulsar wind with $\sigma = 0.03$ (left panel) and $\sigma = 0.1$(right panel).

ACKNOWLEDGMENTS

The authors are grateful to V. Bosch-Ramon for his interest to this study and useful discussions. The work of S.V.Bogovalov have been supported by the Federal Targeted Program "The Scientific and Pedagogical Personnel of the Innovative Russia" in 2009-2013 (the state contract N 536 on May 17, 2010). The work of A.V.Koldoba and G.V.Ustugova has been supported by RFBR grants Nr. 09-01-00640a and Nr. 09-02-00502a

REFERENCES

Abdo A. A., Ackermann M., Ajello M., Atwood W. B., Axelsson M., Baldini L. et al., 2009a, ApJ, 701, L123

Abdo A. A., Ackermann M., Ajello M., Atwood W. B., Axelsson M., Baldini L. et al., 2009b, ApJ, 706, L56

Abdo A. A., Fermi LAT Collaboration Chernyakova M., Neronov A., Grundstrom E., Fermi Pulsar Timing Consortium t., 2011, ArXiv e-prints

Acciari V. A., Aliu E., Arlen T., Aune T., Beilicke M., Benbow W. et al., 2011, ApJaccepted

Aharonian F., Akhperjanian A. G., Anton G., Barres de Almeida U., Bazer-Bachi A. R., Becherini Y. et al., 2009, A&A, 507, 389

Aharonian F., Akhperjanian A. G., Aye K.-M., Bazer-Bachi A. R., Beilicke M., Benbow W. et al., 2005a, Science, 309, 746

Aharonian F., Akhperjanian A. G., Aye K.-M., Bazer-Bachi A. R., Beilicke M., Benbow W. et al., 2005b, A&A, 442, 1

Aharonian F., Akhperjanian A. G., Bazer-Bachi A. R., Beilicke M., Benbow W., Berge D. et al., 2006, A&A, 460, 743

Albert J., Aliu E., Anderhub H., Antoranz P., Armada A., Asensio M. et al., 2006, Science, 312, 1771

Anderhub H., Antonelli L. A., Antoranz P., Backes M., Baixeras C., Balestra S. et al., 2009, ApJ, 706, L27

Bogovalov, S. V. 1999, A&A, 349, 1017

Bogovalov S., Tsinganos K., 1999, MNRAS, 305, 211

Bogovalov, S. V., & Khangoulian, D. V. 2002, MNRAS, 336, L53

Bogovalov S. V., Chechetkin V. M., Koldoba A. V., Ustyugova G. V., 2005, MNRAS, 358, 705

Bogovalov S. V., Khangulyan D. V., Koldoba A. V., Ustyugova G. V., Aharonian F. A., 2008, MNRAS, 387, 63

Bosch-Ramon V., Barkov M. V., 2011, A&A submitted [astro-ph/1105.6236]

Bosch-Ramon V., Khangulyan D., 2009, International Journal of Modern Physics D, 18, 347

Bucciantini N., 2002, A&A, 387, 1066

Bucciantini N., Amato E., Del Zanna L., 2005, A&A, 434, 189

Chernyakova M., Neronov A., Lutovinov A., Rodriguez J., Johnston S., 2006, MNRAS, 367, 1201

Dubus G., 2006, A&A, 456, 801

Gaensler B. M., Slane P. O., 2006, ARA&A, 44, 17

Johnston S., Manchester R. N., Lyne A. G., Bailes M., Kaspi V. M., Qiao G., D'Amico N., 1992, ApJ, 387, L37

Kennel C. F., Coroniti F. V., 1984a, ApJ, 283, 694

Kennel C. F., Coroniti F. V., 1984b, ApJ, 283, 710

Kerschhaggl M., 2011, A&A, 525, A80+

Khangoulian D. V., Bogovalov S. V., 2003, Astronomy Letters, 29, 495

Khangulyan D., Hnatic S., Aharonian F., Bogovalov S., 2007, MNRAS, 380, 320

Khangulyan D. V., Aharonian F. A., Bogovalov S. V., Koldoba A. V., Ustyugova G. V., 2008, International Journal of Modern Physics D, 17, 1909

Komissarov S. S., Lyubarsky Y. E., 2003, MNRAS, 344, L93

Maraschi L., Treves A., 1981, MNRAS, 194, 1P

Martocchia A., Motch C., Negueruela I., 2005, in L. Burderi, L. A. Antonelli, F. D'Antona, T. di Salvo, G. L. Israel, L. Piersanti, A. Tornambè, & O. Straniero ed., Interacting

Binaries: Accretion, Evolution, and Outcomes Vol. 797 of American Institute of Physics Conference Series, LS 5039 / RX J1826.2-1450: A Young Pulsar?. pp 581–584

McCollum B., 1993, in American Astronomical Society Meeting Abstracts Vol. 25 of Bulletin of the American Astronomical Society, A Pre-Periastron UV Look and Estimate of the Mass Loss Rate of the Be Companion of PSR 1259-63. pp 1321–+

Negueruela I., Ribó M., Herrero A., Lorenzo J., Khangulyan D., Aharonian F. A., 2011, ApJ, 732, L11+

Neronov A., Chernyakova M., 2007, Ap&SS, 309, 253

Paredes J. M., Martí J., Ribó M., Massi M., 2000, Science, 288, 2340

Rees M. J., Gunn J. E., 1974, MNRAS, 167, 1

Stephenson C. B., Sanduleak N., 1971, Publications of the Warner & Swasey Observatory, 1, 1

Uchiyama Y., Tanaka T., Takahashi T., Mori K., Nakazawa K., 2009, ApJ, 698, 911

Ustyugova G. V., Koldoba A. V., Romanova M. M., Chechetkin V. M., Lovelace R. V. E., 1999, ApJ, 516, 221

Vink J. S., de Koter A., Lamers H. J. G. L. M., 2000, A&A, 362, 295